International Journal on Magnetic Particle Imaging
Vol 9, No 1, Suppl 1, Article ID 2303027, 4 Pages

Infinite Science Publishing

Proceedings Article

Adaption of direct Chebyshev reconstruction to an anisotropic particle model

Christine Droigk [a,*] · Marco Maass [a] · Mathias Eulers [a] · Alfred Mertins [a,b]

[a] Institute for Signal Processing, University of Lübeck, Lübeck, Germany
[b] German Research Center for Artificial Intelligence (DFKI), Lübeck, Germany
[*] Corresponding author, email: c.droigk@uni-luebeck.de

Abstract

Model-based image reconstruction in magnetic particle imaging (MPI) is an alternative to common reconstruction methods relying on a measured system matrix. It avoids the time-consuming measurement process but has the problem of inferior image quality due to the complex imaging chain that has to be modeled. Recently, a direct reconstruction method using weighted Chebyshev polynomials for multi-dimensional MPI has been proposed that operates in the frequency domain and even does not need a simulated system matrix. However, as the underlying model neglects several physical processes, including the anisotropy of nanoparticles, artifacts in the reconstructed particle distribution can occur. In this work, an adaption of the direct reconstruction method to an anisotropic particle model is proposed. It is shown that the adaption reduces deformations of the reconstructed particle distribution and thus provides one further step towards fast and high quality model-based image reconstruction.

I. Introduction

Magnetic particle imaging (MPI) is a tomographic imaging modality and can illustrate the distribution of superparamagnetic iron-oxide nanoparticles (SPIONs) inside a field of view (FOV) [1]. Several methods exist to obtain an image reconstruction of the SPION distribution. One common approach is the measurement of the so-called system matrix which then is used to set up a regularized system of linear equations. Its solution is the concentration of the SPION distribution. To avoid the time-consuming measurement process, several alternatives have been proposed. One of these alternatives is the modeling of the physical processes [2–6]. The model can then be used to, e.g., obtain a simulated system matrix [7]. Besides, a direct reconstruction without the use of a system matrix was shown to be possible [8]. The latter exploits the structure of the system function in the spatio-temporal Fourier domain [9] to obtain a relationship between the induced voltage signal and the weighted tensor product of Chebyshev polynomials. The reconstruction method is very fast and memory efficient. However, as the underlying model relies on the Langevin theory of paramagnetism and neglects several physical effects, the quality of the reconstructed images is worse than that of reconstructed images using a measured system matrix. To obtain a better image quality, more complex physical models like [4] are necessary. In [5, 6], an equilibrium model that also includes the effect of anisotropic particles has been presented, and in [10] the relationship of it to the formulation of system function in the frequency domain based on the Langevin model has been exploited. Based on this relationship we propose to adapt the direct Chebyshev reconstruction to the model including anisotropy effects by adjustung the deconvolution step. Our experiments on simulated data show that the image quality can be improved using the proposed adaption in the deconvolution step.

II. Methods and materials

The direct Chebyshev reconstruction (DCR) presented in [8] relies on the formulation of the system function in the Langevin model of paramagnetism [9]. It was shown that in multi-dimensional field-free point (FFP) MPI with a Lissajous trajectory of the FFP, the convolved SPION distribution can be recovered by summing up tensor products of Chebyshev polynomials of second kind and certain order weighted with the frequency components of the measured voltage signal. In a second step, this result has to be rescaled and deconvolved to obtain the final image reconstruction. Here, we consider the two-dimensional case: Let $c : \mathbb{R}^2 \to \mathbb{R}_+$ denote the concentration distribution of the SPIONs, $\mathscr{L}_{z_1,z_2} = \frac{\partial^2}{\partial z_1 \partial z_2}\mathscr{L}(\boldsymbol{z})$ the partial derivative of the two-dimensional Langevin function $\mathscr{L} : \mathbb{R}^2 \to \mathbb{R}^2$ with $\mathscr{L}(\boldsymbol{z}) = \mathscr{L}(\|\boldsymbol{z}\|_2)\frac{\boldsymbol{z}}{\|\boldsymbol{z}\|_2}$ and $\mathscr{L}(z) = \coth(z) - \frac{1}{z}$. In the two-dimensional case, the convolved SPION distribution

$$\tilde{\boldsymbol{c}}(\boldsymbol{x}) = \left(c(\boldsymbol{z}) * \mathscr{L}_{z_1,z_2}(-\beta \boldsymbol{G}\boldsymbol{z})\right)\left(\boldsymbol{G}^{-1}\boldsymbol{A}\boldsymbol{x}\right) \tag{1}$$

can then be approximated by [8]

$$\tilde{\boldsymbol{c}}(\boldsymbol{x}) \approx \sum_{k\in\mathbb{K}} \frac{4|(k-\lambda_k^* N_B)(k-\lambda_k^*(N_B-1))|}{\pi^2\beta^2\det(\boldsymbol{A})}(\boldsymbol{C}_k)^{-1} \boldsymbol{u}_k \mathrm{i}^{\lambda_k^*} U_{|n_k^*|-1}(x_1) U_{|m_k^*|-1}(x_2). \tag{2}$$

Here, the set $\mathbb{K}$ contains certain frequency components, N_B is the frequency divider, $\lambda_k^* = \mathrm{round}\left(\frac{(2N_B-1)k}{(2N_B^2-2N_B-1)}\right)$ is a solution of a certain minimization problem, $\beta \in \mathbb{R}$ is a known constant, $\boldsymbol{C}_k \in \mathbb{R}^{2\times 2}$ is a known matrix, $\boldsymbol{A} \in \mathbb{R}^{2\times 2}$ and $\boldsymbol{G} \in \mathbb{R}^{2\times 2}$ are matrices containing the amplitudes and gradients of the magnetic fields, $\boldsymbol{u}_k$ is the k-th frequency component of the Fourier transformed voltage signal, and $U_n : \mathbb{R} \to \mathbb{R}$ are Chebyshev polynomials of second kind and order $n \in \mathbb{N}$.

When now considering the model including uniaxial anisotropy [5, 6], the convolution in (1) changes to [10]

$$\tilde{\boldsymbol{c}}(\boldsymbol{x}) = \left(c(\boldsymbol{z}) * \frac{\partial^2}{\partial z_1 \partial z_2}\mathscr{E}(-\beta\boldsymbol{G}\boldsymbol{z}, \alpha_{K_{\mathrm{anis}}}(\boldsymbol{x}), \boldsymbol{n}(\boldsymbol{x}))\right)\left(\boldsymbol{G}^{-1}\boldsymbol{A}\boldsymbol{x}\right). \tag{3}$$

Instead of the Langevin function, the kernel $\mathscr{E} : \mathbb{R}^2 \times \mathbb{R} \times \mathbb{S}^2 \to \mathbb{R}^2$ is assumed which is the first moment of the probability density function of the magnetic moment of a SPION in the equilibrium model with uniaxial anisotropy. Here, $\mathbb{S}^2$ is the surface of the unit sphere, $\alpha_{K_{\mathrm{anis}}} : \mathbb{R}^2 \to \mathbb{R}$ denotes the strength of the anisotropy and $\boldsymbol{n} : \mathbb{R}^2 \to \mathbb{S}^2$ is the easy axis of the particle anisotropy. Both $\boldsymbol{n}(\boldsymbol{x})$ and $\alpha_{K_{\mathrm{anis}}}(\boldsymbol{x})$ are considered to be time invariant. Thus, the original concentration c can be obtained by deconvolving $\tilde{\boldsymbol{c}}$ with $\frac{\partial^2}{\partial z_1 \partial z_2}\mathscr{E}$ instead of $\mathscr{L}_{z_1,z_2}$. Be aware that $\mathscr{E}$ depends on the position $\boldsymbol{x}$. This means that it can be seen as a spatially varying kernel. For details on $\mathscr{E}$ and its calculation, we refer to [10].

For the adapted reconstruction, we now consider the discretizations of all continuous functions. Thus, for the deconvolution, a convolution matrix $\boldsymbol{M} \in \mathbb{R}^{2N\times N+M-1}$ can be set up that contains in each row the kernel $\frac{\partial^2}{\partial z_1 \partial z_2}\mathscr{E}$ evaluated at the corresponding spatial position. Here, N is the number of considered spatial positions of the drive-field field of view and M is the number of spatial positions at which the kernel $\frac{\partial^2}{\partial z_1 \partial z_2}\mathscr{E}$ is evaluated. The matrix $\boldsymbol{M}$ can be set up by joining two other matrices. Let $\boldsymbol{M}_x \in \mathbb{R}^{N\times N+M-1}$ denote the convolution matrix for the x receive path and $\boldsymbol{M}_y \in \mathbb{R}^{N\times N+M-1}$ the convolution matrix for the y receive path. Note that the corresponding kernel components are the transposed components of the other receive paths, so that only one component has to be computed and saved to set up both convolution matrices $\boldsymbol{M}_x$ and $\boldsymbol{M}_y$. Let $\boldsymbol{c}_d \in \mathbb{R}_+^N$ denote the discretized concentration vector and $\tilde{\boldsymbol{c}}_{1,d}, \tilde{\boldsymbol{c}}_{2,d} \in \mathbb{R}^N$ denote the discretized vector of the first and second component of the convolved concentration that is reconstructed by the DCR method. The final minimization problem then reads

$$\min_{\boldsymbol{c}_d} \left\| \begin{pmatrix} \boldsymbol{M}_x \\ \boldsymbol{M}_y \end{pmatrix} \boldsymbol{c}_d - \begin{pmatrix} \tilde{\boldsymbol{c}}_{1,d} \\ \tilde{\boldsymbol{c}}_{2,d} \end{pmatrix} \right\|_2^2 + \lambda R(\boldsymbol{c}_d). \tag{4}$$

Here, $\lambda \in \mathbb{R}_+$ is a regularization parameter and $R : \mathbb{R}^N \to \mathbb{R}_+$ the regularization function. To obtain a direct reconstruction and thus to avoid the use of iterative algorithms, the choice $R(\boldsymbol{c}_d) = \|\boldsymbol{c}_d\|_2^2$ can be made which leads to the analytical solution $\boldsymbol{c}_d = (\boldsymbol{M}^\top\boldsymbol{M} + \lambda\boldsymbol{I})^{-1}\boldsymbol{M}^\top(\tilde{\boldsymbol{c}}_{1,d}^\top, \tilde{\boldsymbol{c}}_{2,d}^\top)^\top$.

III. Experiments

To test the isolated impact of anisotropy effects on the direct reconstruction method and the effect of the adapted deconvolution, numerical simulations with a simulated system matrix were performed. The system matrix was simulated including anisotropy effects. For this, the equilibrium model including uniaxial anisotropy effects [5, 6] was used. This model is based on [4], but assumes an equilibrium solution. Following the results of [4], the easy axis $\boldsymbol{n}(x) = \frac{\boldsymbol{H}^S(\boldsymbol{x})}{\|\boldsymbol{H}^S(\boldsymbol{x})\|_2^2}$ is aligned at the selection field $\boldsymbol{H}^S(\boldsymbol{x})$ and the anisotropy strength is spatially varying with $\alpha_{K_{\mathrm{anis}}}(\boldsymbol{x}) = \frac{g_{K_{\mathrm{anis}}} V_C}{k_B T_B}\frac{\|\boldsymbol{H}^S(\boldsymbol{x})\|^2}{\max_{x\in\Omega}\|\boldsymbol{H}^S(\boldsymbol{x})\|^2}$ with the anisotropy gradient $g_{K_{\mathrm{anis}}} = 1250\,\mathrm{Jm}^{-1}$. Besides, the particle volume is chosen as $V_C = \frac{\pi}{6}(25\cdot 10^{-9})^3\,\mathrm{m}^3$, the particle temperature is set to $T_B = 300\,\mathrm{K}$, the Boltzmann constant is denoted as k_B,and Ω is the FOV. The induced voltage signal of the phantom in Fig. 1 was simulated via multiplication of the simulated system matrix with the concentration vector of the SPION distribution of the phantom. Then, the first step of the DCR was performed to obtain the convolved concentration vectors $\tilde{c}_{1,d}$ and $\tilde{c}_{2,d}$, i.e. (2) was evaluated. Then, the deconvolution with the spatially varying kernel was performed, i.e. (4) was solved. The

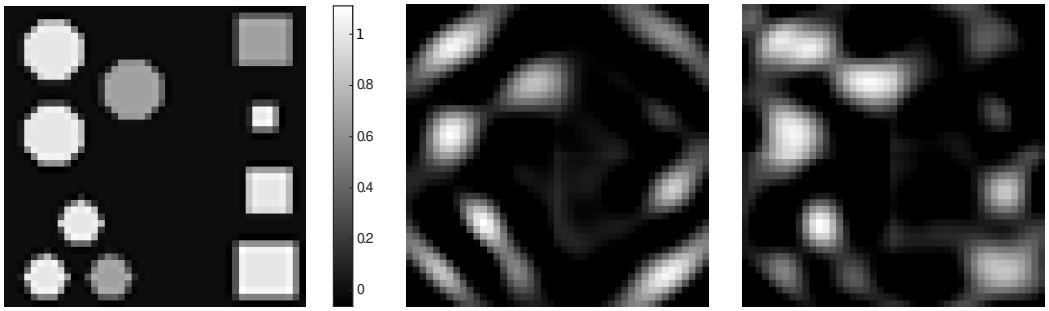

Figure 1: Ground-truth concentration phantom (left) and direct reconstruction results with deconvolution assuming the underlying Langevin kernel $\mathscr{L}_{z_1,z_2}$ (middle) and assuming the underlying spatially varying kernel $\frac{\partial^2}{\partial z_1 \partial z_2}\mathscr{E}$ (right). The SSIM is stated below. As the simulation considers the particle anisotropy, the deconvolution with the Langevin kernel leads to deformations of the phantom elements. The kernel $\frac{\partial^2}{\partial z_1 \partial z_2}\mathscr{E}$ considers those effects and thus leads to a better resolution of the phantom shapes. Note that in [8] no particle anisotropy was considered in the simulations which is why those effects did not occur.

size of the kernel was chosen to be the size of the drive-field FOV, which is $M = N = 45 \cdot 45$ and covers a size of 24 mm × 24 mm. A Tikhonov regularization was used allowing an analytical solving, and the parameter λ was optimized. For comparison purpose, the obtained vectors $\tilde{\boldsymbol{c}}_{1,d}, \tilde{\boldsymbol{c}}_{2,d}$ were also deconvolved assuming the Langevin kernel $\mathscr{L}_{z_1,z_2}$ as proposed in [8]. The structural similarity (SSIM) [11] was computed for both reconstruction results. Besides, the reconstruction time for both methods is measured and compared with the reconstruction time of a system matrix approach with a Kaczmarz algorithm using 10 iterations.

IV. Results and discussion

The obtained reconstruction results are shown in Fig. 1. Besides, also the obtained SSIM indices are stated below the reconstruction images. It is visible that, when anisotropy effects are involved in the signal generation but not considered in the reconstruction, there arise deformations of the original shapes. This effect is the larger the closer the SPIONs are located to the image corners. At these locations also the anisotropy strength is the largest following the considered model. When using an adjusted kernel for the deconvolution which considers the anisotropy effects, the deformations become considerably less: In the right reconstruction image in Fig. 1, the shape of the circles and the squares are matching the original phantom much better than the reconstruction in the middle. This is also reflected in the higher SSIM index. The reconstruction quality could be improved, but the proposed method has drawbacks regarding the reconstruction speed and the memory consumption. In Table 1, an overview of the reconstruction time of the DCR based on the Langevin model (DCR-L), the system matrix approach with 10 iterations of Kaczmarz algorithm (SM-Kacz-10) and the proposed DCR assuming uniaxial anisotropy (DCR-A) is given. The proposed DCR-A is the slowest of the tested methods while the DCR-L is by far the fastest. Due to the used spatially varying kernel, the deconvolution can no longer be performed efficiently in the Fourier domain. Therefore, a convolution matrix has to be set up which has a larger memory consumption. Because the matrix is larger and less sparse than the multiplication matrix used in the Fourier domain in [8], the analytical solution of the linear system of equations in (4) with a Tikhonov regularization consumes more time. Compared to the direct reconstruction based on the Langevin model, instead of one kernel of the size M now N kernels of size M are stored. Whether the size of a system matrix containing $2NK$ entries is larger depends on the relation of M and K. Therefore, to achieve a meaningful use of the proposed method, the memory consumption and reconstruction time must be reduced. However, this seems to be quite possible: The used kernel $\frac{\partial^2}{\partial z_1 \partial z_2}\mathscr{E}$ is very similar in neighboring areas. Therefore it seems feasible to reduce the number of spatial positions at which the kernel is saved without large losses in reconstruction quality. Then, a patch-wise deconvolution performed in the Fourier domain might be possible that saves time and memory. Further speedup without

Table 1: Reconstruction time for the system matrix approach using Kaczmarz algorithm with 10 iterations (SM-Kacz-10), the DCR using the Langevin kernel for deconvolution (DCR-L), and the DCR with the spatially varying kernel used for deconvolution (DCR-A).

Method	SM-Kacz-10	DCR-L	DCR-A
Reconstr. time	0.23 s	0.02 s	1.41 s

10.18416/ijmpi.2023.2303027

adjusting the method would also be conceivable by performing a one-time singular value decomposition on $\boldsymbol{M}$, thus greatly speeding up the solution of the system of equations in (4) for future reconstructions.

For the application to real-world measurements, reasonable model parameters must be chosen and the impact of the signal chain of the MPI scanner must be considered, e.g. via the estimation of a transfer function as done in [7]. The parameter choice used in the experiments were those of [4]. In [4], they were used to simulate a system matrix that was shown to be very close to real-world measurements. Using this reasonable parameter choice, the kernel $\mathscr{E}$ can be computed and the only difference in the reconstruction of real-world measurements is then to correct the voltage signal for the scanner's receive chain via, e.g., the division of the estimated transfer function. If one wants to further optimize the parameter choice of the underlying model, this can be done by comparing differently simulated system matrices and a measured system matrix, as done in [4].

V. Conclusion

An adaption of the DCR [8] to a more complex model including anisotropy effects has been prosposed that uses the insights of [10]. To this end, the deconvolution step was modified and a spatially varying kernel was used instead of the partial derivative of the Langevin function. The simulations show that this modification leads to a better reconstruction of the shape of the SPION distribution at the border of the FOV, when anisotropy effects have been regarded in the simulation of the induced voltage signal. The main drawback is the higher time and memory consumption due to the processing and storage of the spatially varying kernel. Future research on a patch-wise deconvolution in the Fourier domain might overcome this drawback.

Author's statement

Conflict of interest: Authors state no conflict of interest.

References

[1] B. Gleich and J. Weizenecker. Tomographic imaging using the nonlinear response of magnetic particles. *Nature*, 435(7046):1214–1217, 2005, doi:10.1038/nature03808.

[2] J. Rahmer, J. Weizenecker, B. Gleich, and J. Borgert. Signal encoding in magnetic particle imaging: Properties of the system function. *BMC medical imaging*, 9(1):1–21, 2009.

[3] T. Kluth. Mathematical models for magnetic particle imaging. *Inverse Problems*, 34(8):083001, 2018.

[4] T. Kluth, P. Szwargulski, and T. Knopp. Towards accurate modeling of the multidimensional magnetic particle imaging physics. *New Journal of Physics*, 21(10):103032, 2019.

[5] H. Albers and T. Kluth. Immobilized nanoparticles with uniaxial anisotropy in multi-dimensional Lissajous-type excitation: An equilibrium model approach. *International Journal on Magnetic Particle Imaging*, 8(1 Suppl 1), 2022.

[6] M. Maass, C. Droigk, M. Eulers, and A. Mertins. An analytical equilibrium solution to the Néel relaxation Fokker-Planck equation. *International Journal on Magnetic Particle Imaging*, 8(1 Suppl 1), 2022, doi:10.18416/IJMPI.2022.2203008.

[7] T. Knopp, S. Biederer, T. F. Sattel, J. Rahmer, J. Weizenecker, B. Gleich, J. Borgert, and T. M. Buzug. 2D model-based reconstruction for Magnetic Particle Imaging. *Medical Physics*, 37(2):485–491, 2010.

[8] C. Droigk, M. Maass, and A. Mertins. Direct multi-dimensional Chebyshev polynomial based reconstruction for Magnetic Particle Imaging. *Physics in Medicine & Biology*, 67(4):045014, 2022.

[9] M. Maass and A. Mertins. On the Representation of Magnetic Particle Imaging in Fourier Space. *International Journal on Magnetic Particle Imaging*, 6(1):1–21, 2020, doi:10.18416/IJMPI.2019.1912001.

[10] M. Maass, C. Droigk, M. Eulers, and A. Mertins. A system function component model for magnetic particle imaging with anisotropic particles. *International Journal on Magnetic Particle Imaging*, 9(1 Suppl 1), 2023, doi:10.18416/IJMPI.2023.2303076.

[11] Z. Wang, A. C. Bovik, H. R. Sheikh, and E. P. Simoncelli. Image quality assessment: From error visibility to structural similarity. *IEEE Transactions on Image Processing*, 13(4):600–612, 2004.